Available online at www.sciencedirect.com
ScienceDirect
Trans. Nonferrous Met. Soc. China 29(2019) 1610−1620
Transactions of Nonferrous Metals Society of China
www.tnmsc.cn

Metallurgical behavior and variation of vibro-acoustic signal during preheating assisted friction stir welding between AA6061-T6 and AA7075-T651 alloys

Ashu GARG, Madhav RATURI, Anirban BHATTACHARYA

Department of Mechanical Engineering, Indian Institute of Technology Patna, Bihar, India

Received 17 November 2018; accepted 17 May 2019

Abstract: The present work investigated the effects of pin profiles (cylindrical and square), pin eccentricity (0.5 mm and 1 mm) in cylindrical tool and preheating (secondary heating) on metallurgical behavior, variation of vibro-acoustic signal pattern and joint strength during friction stir welding (FSW) between AA6061-T6 and AA7075-T651 alloys. The eccentric tool pins were observed to provide good flowability and intermixing between dissimilar metals, increased the size of stir zone, and the grains in stir zone were sufficiently finer with eccentric tool pin than concentric pin. The magnitude of vibro-acoustic signal increased when shoulder plunging started and drop in signal was noted when the tool shoulder reached its desired depth. The signal magnitude was noted to be higher in welding stage compared to tool plunging stage as the tool took in fresh material during tool movement along the weld path. Preheating the workpiece prior to pin plunging and during welding notably influenced the flow behavior and mixing pattern, and the grains in stir zone were slightly coarser than those in specimen without preheating. Significant reduction in the magnitude of the signal was also observed after preheating. Tensile and flexural strength of joints were also improved slightly when additional heating was employed.

Key words: friction stir welding; tool pin profile; eccentricity; preheating; vibro-acoustic signal; microstructure; strength

1 Introduction

Aluminum alloys are lightweight materials widely used in industries like automotive, aerospace, railways and shipbuilding. In many applications, Al alloys are joined by friction stir welding (FSW), a solid-state welding process developed originally for these difficult-to-fusion weld materials [1,2]. Beyond Al alloys, the materials like Cu alloys, Mg alloys, some steels or metal matrix composites are also joined by this solid-state welding process [1−3]. FSW utilizes the heat generated due to the friction among a rotating tool, pin and workpiece surface as well as plastic deformation of the workpiece [4]. FSW is capable of producing sound quality similar and dissimilar joints; however, the selection of optimum process parameters like rotational speed of tool, traverse speed, and tool pin profiles is important as they influence the material flow, intermixing, and joint strength. RATURI et al [5] studied the effect of tool rotational and traverse speeds, tool pin profiles and preheating during dissimilar FSW of AA6061-T6 and AA7075-T651 and reported that the pin profiles, rotational and traverse speeds have a significant effect on quality and strength of the joint. VERMA et al [6] studied the influence of tool rotational and transverse speeds on mechanical properties, corrosion behavior and microstructure during FSW of AZ31B magnesium alloy and Al6061 aluminum alloy. The influences of different tool pin profiles, tool tilt angles, rotational and welding speeds were investigated by SHANAVAS and EDWIN RAJA DHAS [7] during FSW of AA5052-H32 and they concluded that the joint prepared with tool with tapered square pin profile and intermediate process parameter settings had higher strength. SHARMA et al [8] also performed FSW of AA7039 aluminum alloy with different tool rotational and welding speeds and observed that better strength was obtained with higher level of rotational speed and lower level of welding speed. DAWOOD et al [9] examined different small tool pin profiles (triangular, square and threaded tapered cylindrical) on weld properties and microstructure during FSW of AA6061. They reported that the joint produced by triangular tool pin displayed the best metallurgical behavior, the highest tensile strength and hardness whereas square tool pin displaced

Corresponding author: Anirban BHATTACHARYA; E-mail: abhatta@iitp.ac.in
DOI: 10.1016/S1003-6326(19)65068-5

the least strength. YANG et al [10] studied the effect of different pin profiles and shoulder features on heat generation, microstructure and tensile strength during FSW of AA6061-T6. YADUWANSHI et al [11] analyzed the influence of tool offset during FSW between pure copper and 1100 aluminum alloy and reported that the tool offset towards Al side (by 2 mm) along with plasma heat source produced better joints. JAYABALAKRISHNAN and BALASUBRAMANIAN [12] studied the effect of two different tool pins (normal and offset) during FSW of copper and 6061-T6 aluminum alloys where FSW was performed in linear and eccentric weave pattern, and observed sound weld with offset pin moving in eccentric weave pattern. The influence of different tool pins such as offset pin, concentric pin, half pin and arched pin was investigated on force variation during FSW of AA5083 and minimum forces were obtained for tool with offset pin [13]. The influence of tool pin eccentricity (0.1, 0.2, 0.3 and 0.4 mm) on mechanical properties and microstructure was studied during FSW of AA7075-O alloy [14] wherein the highest tensile strength and elongation, finest grains and best joint quality were obtained for joints prepared with 0.2 mm eccentric tool pin. SHAH et al [15] also reported that eccentric tool pin (0.2 mm eccentricity) improved the material flow in nugget zone and also slightly improved the tensile strength and elongation of AA6061-T651 FSW joints. CHEN et al [16] analyzed the effect of pin eccentricity (0, 0.4 and 0.8 mm) on microstructure and mechanical properties of friction stir processed AA5052 joints. They reported that the eccentric pin enhanced the material flow, refined the grain structure and improved the mechanical strength of joints. They also observed that the excessive eccentricity produced more heat in stir zone which deteriorated the grain structure and mechanical strength. BANG et al [17] investigated gas tungsten arc welding assisted FSW between STS304 and Al6061-T6 and observed that preheating improved the material flow and tensile strength. YADUWANSHI et al [18] investigated the effect of preheating by plasma arc on mechanical properties and microstructure of friction stir welded AA1100 and observed that preheating increased the joint tensile strength and reduced the plunging force. The effect of preheating on axial force and microstructure was also investigated by SINCLAIR et al [19] during FSW of AA6061-T6, and it was reported that preheating improved the plastic flow and reduced the axial flow during welding. The effect of post weld heat treatment and initial temper condition (O and T6) on joint properties was investigated during FSW of similar AA6061 [20], similar AA7075 [21] and dissimilar AA6061−AA7075 alloys [22]. It was reported that the post weld heat treatment improved the joint strength for both temper conditions whereas hardness of joints with O condition significantly improved and some loss in hardness was observed for T6 condition. SAFARBALI et al [23] reported that the post weld treatment improved the tensile strength of dissimilar AA2024-T4 and AA7075-T6 friction stir welds. ÇAM et al [24] examined the influence of addition of inter-layer material (AA7075-T6) and external cooling on joint properties of AA6061-T6 friction stir weld. They reported that the joint obtained using interlayer material did not provide higher tensile strength but hardness of dynamically recrystallized zone increased. DONATUS et al [25] studied the elemental composition across the weld zone during FSW between AA6082-T6 and AA5083-O alloys and reported that the stir zone mainly comprised the material from retreating side of the weld. Researchers also proposed several signal monitoring techniques for FSW or friction stir spot welding (FSSW) process. CHEN et al [26] presented acoustic emission signal analysis using wavelet transform for in-process monitoring of FSW of 6061 aluminum alloy to study the existence, location and size of defects. The effect of different tool profiles on acoustic signals was monitored during FSW of aluminum alloy [27,28], and it was reported that signals generated can effectively be used to characterize the change in pin profiles. The correlation between vibro-acoustic signal and process parameters (dwell time, tool rotational speed and torque) was studied by MACÍAS et al [29] during FSSW between pure copper and 1050-H24 aluminum alloy. It was reported that the vibro-acoustic signal based method can successfully be used for online monitoring of FSSW process. SOUNDARARAJAN et al [30] also analyzed the influence of the plunge depth, traverse and rotational speeds on vibro-acoustic signal pattern during FSW of AA6061. They reported that the amplitude of signal is sensitive to the depth of penetration and signal disappears when the tool losses contact with the workpiece. OROZCO et al [31] presented mathematical model to optimize the parameter setting using vibro-acoustic signal data during FSW of AA1050-H24. RAJAPRAKASH et al [32] also developed a model for in-process monitoring of FSW to detect the occurrence of defects using acoustic emission techniques. In another work, MURTHY et al [33] studied the applicability of acoustic emission technique using image processing parameters to identify the defects during FSW process. They observed that both signal parameters and image processing parameters followed similar trend for same input process parameters.

Aforesaid literatures summarized that the different process parameters and tool pin profiles significantly affect the material flow, intermixing and consequently the strength of the FSW joints. In FSW process, the tool

pin is completely plunged/inserted into the workpiece and difficult to monitor the status/quality of tool during the process. During FSW, the amount of forces experienced by the tool reduces when preheating is employed and expected to improve the material flow/intermixing which may alter the vibro-acoustic signal behavior. Thus, the present work focused on studying the metallurgical behavior in the weld seam and analyzing vibro-acoustic signal during dissimilar FSW between AA6061-T6 and AA7075-T651 using different pin profiles namely concentric cylindrical pin, square pin and eccentric cylindrical pin (0.5 and 1 mm offset) along with the effect of preheating. Microstructural studies using optical and field emission scanning electron microscope were carried out to observe the formation of different zones, material flow pattern, tunnel defects and grains size distribution. Tensile, flexural strength tests of welded joints were also performed and results were reported.

2 Experimental

AA6061-T6 and AA7075-T651 aluminum alloys plates with a thickness of 6.1 mm were cut to dimensions 120 mm (length) × 100 mm (width) and placed in butt configuration for dissimilar FSW using vertical milling machine. Tool rotational speed of 660 r/min, weld traverse speed of 63 mm/min, and pin plunge depth of 5.9 mm followed by shoulder plunging around 0.1 mm were maintained constant for all the experiments. Experimental setup with acoustic signal monitoring and preheating arrangement, welded specimen for tensile, flexural tests and microstructure observation and schematic representation of different tools are shown in Fig. 1. FSW tools were prepared from H13 die steel and dimensions of tools are shown in Fig. 1(c). Tools were designed with two different pin profiles i.e. cylindrical with pin diameter of 6 mm and square with diagonal of 6 mm. Tools with eccentric cylindrical tool pins were prepared to provide eccentricities of 0.5 and 1.0 mm with respect to the tool center.

Additional heating (preheating) of workpiece was provided with the help of butane gas torch prior to plunging and during welding (torch traveled ahead of the FSW tool). Thus, the additional heating acts as a secondary heat source rather than the primary heat generated by virtue of the process. The photographic view of FSW process with preheating arrangement is shown in Fig. 1(a). An in-process vibro-acoustic signal capturing system was employed to record and study the influence of different pin profiles, pin eccentricity and preheating during dissimilar FSW of AA6061-to-AA7075 alloys. Triaxial miniature piezoelectric accelerometer sensor was used to capture vibro-acoustic signals using data acquisition system at a sampling rate of 4.096 kHz. The optical and field emission scanning electron microscopes (FE-SEM) were used for metallographic examinations. Polished specimens were etched with Poulton's reagent (prepared with 20 mL HCl, 35 mL HNO_3, 1.25 mL HF, 1.25 mL distilled water and 20 mL chromic acid solution) for 15 s. Two specimens for tensile and flexural (three-point bending) tests were cut from each of the welded samples with the help of wire electric discharge machining. The tensile and

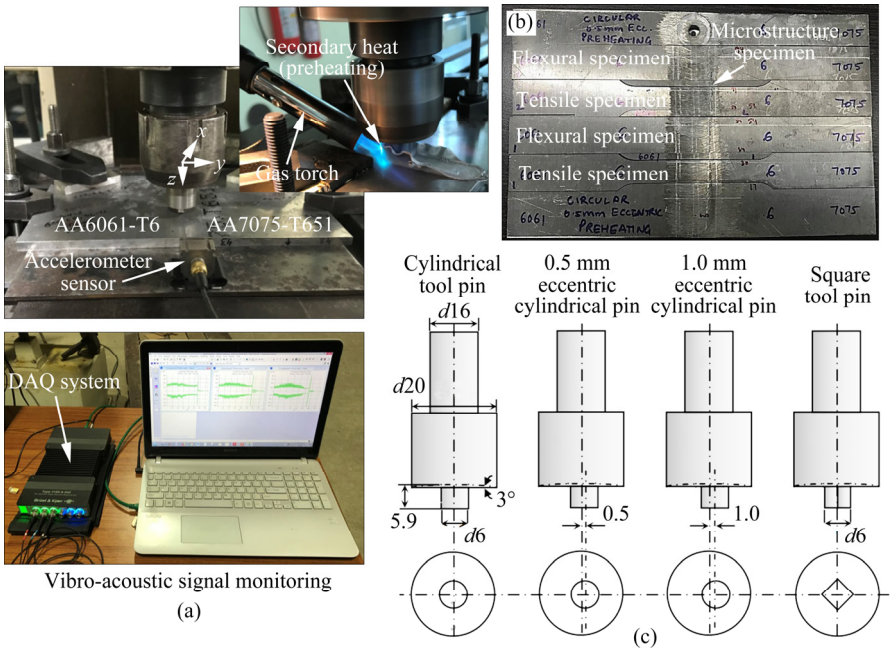

Fig. 1 Experimental setup with acoustic signal monitoring and preheating arrangement (a), welded specimen for tensile, flexural tests and microstructure observation (b) and schematic representation of different tools (unit: mm) (c)

flexural tests were performed on the universal testing machine at cross-head speed of 0.5 mm/min for tensile testing and 1 mm/min for three-point bend (flexural) test.

3 Results and discussion

For metallurgical analysis of welded joints the microscopic images were captured from the location of the specimen as marked in Fig. 1(b) to view the cross-section of FSW welds prepared with cylindrical, eccentric and square tool pins. Microstructures of joint cross-sections prepared with different tool pins at the selected process parameter setting for both without and with preheating are shown in Fig. 2.

Since the FSW is supposed to have a continuous shear and extrusion action, the material flow, intermixing between dissimilar metals, and heat generation are significantly affected by the tool pin profiles. Figure 2 indicates that among different tools used, the tool with eccentric pins causes good stirring/mixing between the dissimilar metals, leading to the formation of larger size stir zone (larger for 1 mm eccentric pin, Fig. 2(c)) in welded joint compared to stir zone (SZ) with concentric tool pins (both circular and square). The microstructure of weld cross-section obtained with square tool pin is shown in Fig. 2(d). For square tool pin due to pulsating action of rotating tool pin, the stronger stirring and mixing of plasticized material is observed. The square tool pin sweeps high viscosity material from plasticized zone under the action of tool rotation as illustrated schematically in Fig. 2(e). Figure 2 also shows that the size of the SZ formed with square tool pin is moderately larger than that of the SZ formed with concentric cylindrical tool pin (without eccentricity). Also, the size of tunnel formed with square tool pin is observed to be slightly smaller than that formed with cylindrical tool pin due to stronger stirring and pulsating action of rotating square tool pin. The microstructures of welded joints

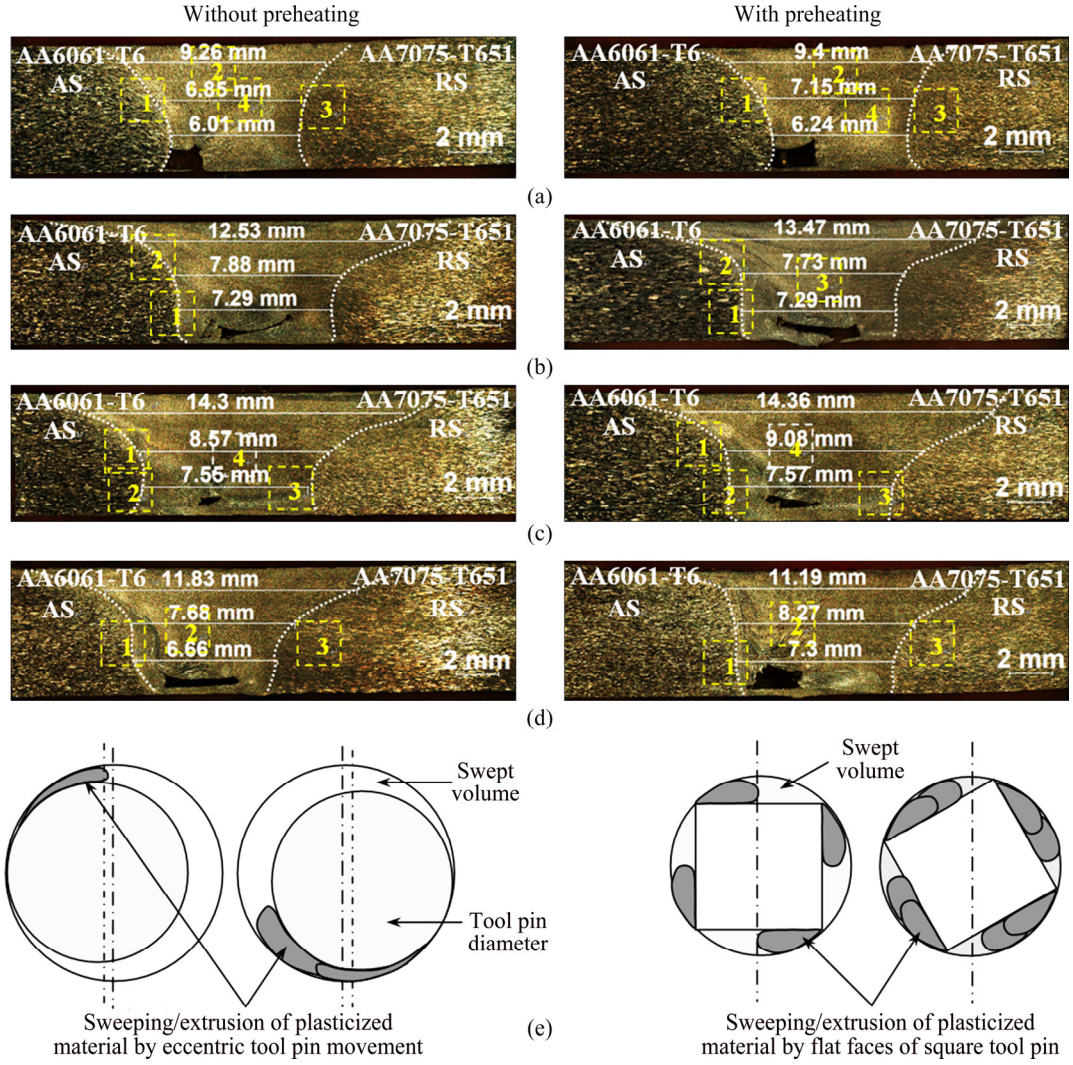

Fig. 2 Micrographs on weld cross-sections of joints obtained using cylindrical tool pin (a), cylindrical tool pin with eccentricity of 0.5 mm (b), cylindrical tool pin with eccentricity of 1 mm (c), square tool pin (d) and schematic illustration of material flow around eccentric and square tool pin (e) (Regions marked in figure are separately analyzed through FE-SEM)

obtained when preheating (secondary heat source) was employed are also shown in Fig. 2. The additional heating helps for easy deformation and higher volume of plasticized material starts flowing around the tool pin profile. Therefore, the size of SZ is slightly larger than that of the case when no preheating is used. The microstructure examination of cross-section also shows that with preheating the amount of material from retreating side (RS), i.e. AA7075-T651 stirred in SZ, is little more than that of the specimen without any preheating. This is mainly due to the easy extrusion of plasticized material from RS to SZ. Preheating also causes better intermixing and interlocking between AA6061 and AA7075 alloys, which improve the weld quality and strength.

Furthermore, metallurgical analyses were also carried out by SEM study of the cross-section of FSW joints prepared with different tool pins to observe the formation of different zones, material flow, intermixing of dissimilar metals and grains distribution for both without and with preheating. The SEM images on the cross-sections of dissimilar AA6061−AA7075 joints friction stir welded with cylindrical tool pin are shown in Fig. 3. Figure 3 shows the finer grain structure in SZ for both cases without and with preheating (Region 1) as compared to other zones due to stirring and dynamic recrystallization of grains analogous with high frictional thermal cycle and strain rate. The finer grains are also observed in the thermo-mechanically affected zone (TMAZ) as compared to the heat affected zone (HAZ) associated with moderate thermal cycle and strain rate. It may also be noted from Fig. 3(a) that the microstructure of SZ (Region 4) is characterized by two distinct grain structures, i.e. the grains of AA6061-T6 are coarser than those observed in AA7075-T651. For the case without preheating the grain size at distribution peak was measured to be 8.37 μm in AA6061-T6 region whereas grain size in AA7075-T651 region was measured to be 5.98 μm. Figure 3(a) (Region (3)) also shows the large elongated grains in HAZ region of RS (AA7075-T651)

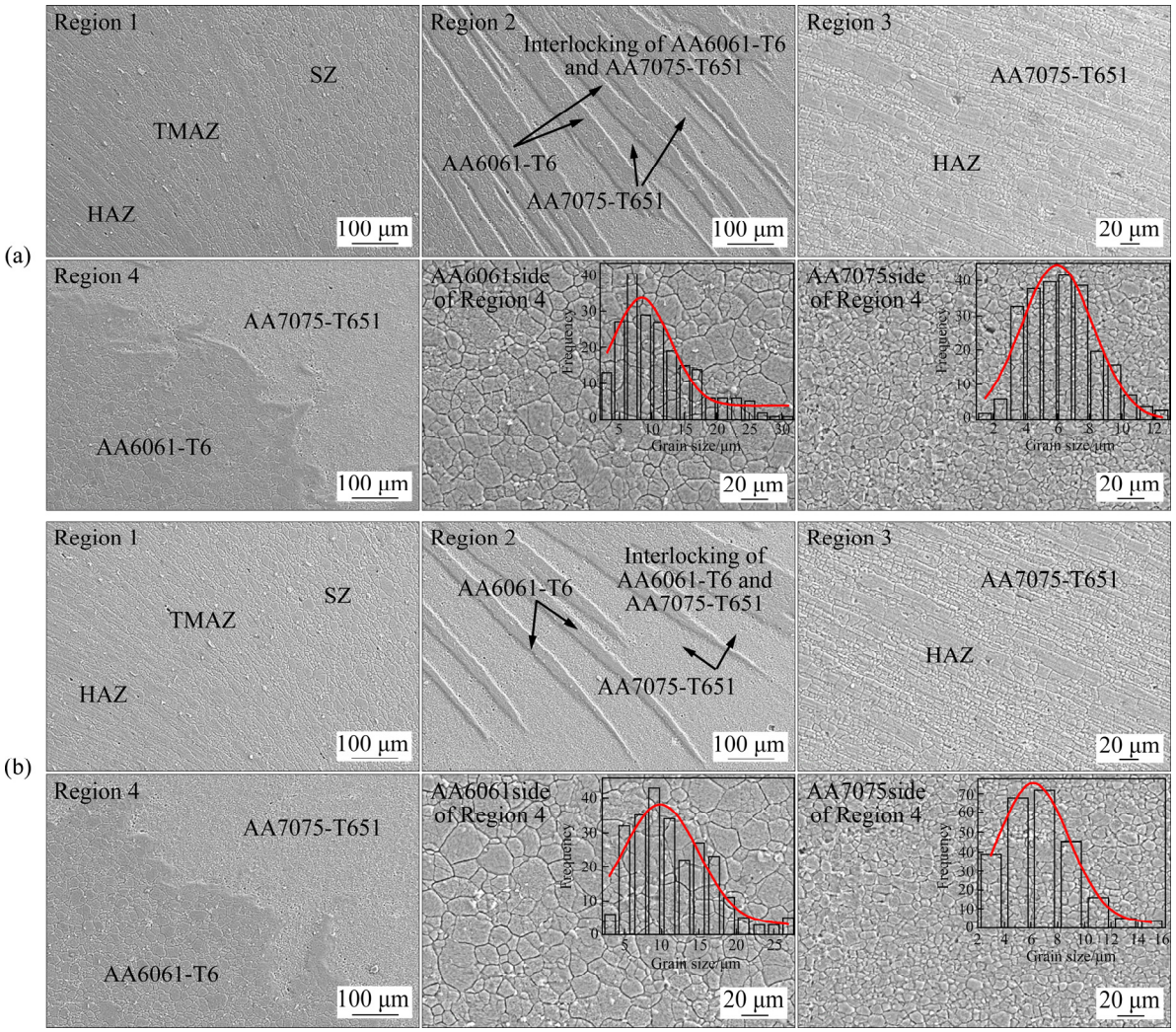

Fig. 3 FE-SEM images of different regions on cross-sections of AA6061−AA7075 FSW joint obtained using cylindrical tool pin: (a) Without preheating (referring to Fig. 2(a) for locations of Regions 1, 2, 3 and 4); (b) With preheating (referring to Fig. 2(a) for locations of Regions 1, 2, 3 and 4)

that are broken into fine and equiaxed grains associated with stronger stirring and aligned along the material flow direction. The mixing and interlocking between AA6061 and AA7075 at different locations (Region 2 and Region 4) are also observed for both cases without and with preheating. Further examination of grain structure also reveals that the grain distribution/size in preheated specimen is quite comparable or slightly coarser than the grains observed in specimen prepared without preheating. Preheating with additional heat source causes the coarsening of precipitate distribution in SZ and slight increase in grain size is noticed. For the joint specimen prepared with preheating the grain size at distribution peak was measured to be 9.83 μm in AA6061-T6 region and in AA7075-T651 region grain size was measured to be 6.17 μm.

Figure 4 shows the FE-SEM images of AA6061−AA7075 dissimilar FSW joint cross-section welded with cylindrical tool pin with a eccentricity of 0.5 mm. In eccentric tool pin due to larger sweeping area compared to concentric tool pin, more heat is expected to generate due to both friction and plastic deformation of the workpiece. Plasticized material starts flowing around the tool pin surface due to extrusion/sweeping action by eccentric tool pin (shown schematically in Fig. 2(e)) that causes good mixing and interlocking between dissimilar metals. FE-SEM images from Region 1 and Region 2 of Fig. 2(b) shown in Fig. 4(a) indicate the formation of onion ring pattern in SZ due to extrusion action of an eccentric pin. The TMAZ region on the advancing side (AS) (Region 2, Fig. 4(a)) can be clearly identified from the SZ and HAZ characterized by a difference in grain size. The grains in TMAZ are observed to be elongated and aligned along the material flow direction.

The FE-SEM images of the cross-section of AA6061−AA7075 FSW joint obtained with 1 mm eccentric cylindrical tool pin are shown in Fig. 5. In 1 mm eccentric tool pin due to the larger sweeping area, intensive stirring/mixing between dissimilar metals and large amount of heat are expected. Rotation of the eccentric tool pin causes extrusion action of the plasticized material in a sequential manner and consequently an onion ring pattern is formed in the SZ. The contrast between the onion ring patterns represents the presence of AA6061-T6 and AA7075-T651 in the SZ and better mixing/interlocking between AA6061 and AA7075 can improve the joint strength. Finer grains in SZ are observed in joint prepared with 1 mm eccentric tool pin wherein the grain size at distribution peak is measured to be 6.18 μm in AA6061-T6 region and 3.60 μm in AA7075-T651 region when no preheating is used. For the joint prepared with preheating the grain size in SZ is measured to be 6.80 and 3.99 μm respectively in AA6061 and AA7075 regions.

Figure 6 shows the FE-SEM images of AA6061−AA7075 friction stir joint cross-section welded with square tool pin. For square tool pin due to pulsating action, stronger stirring and mixing of plasticized material took place as compared to concentric cylindrical tool pin. Figure 6 (Region 1) also shows the formation of onion ring pattern in SZ associated with the extrusion or pulsating action of flat faces of tool pin in which number of layers are extruded by the rotating tool pin. The grains in this region are observed to be finer due to the dynamic recrystallization of the grains. The microstructure of SZ is observed to be finer as compared to the joints prepared with concentric cylindrical pin but slightly coarser than the eccentric tool pin. For square tool pin, the grain size (at distribution peak) in SZ of welded joint obtained without preheating is measured to be 6.74 and 3.83 μm

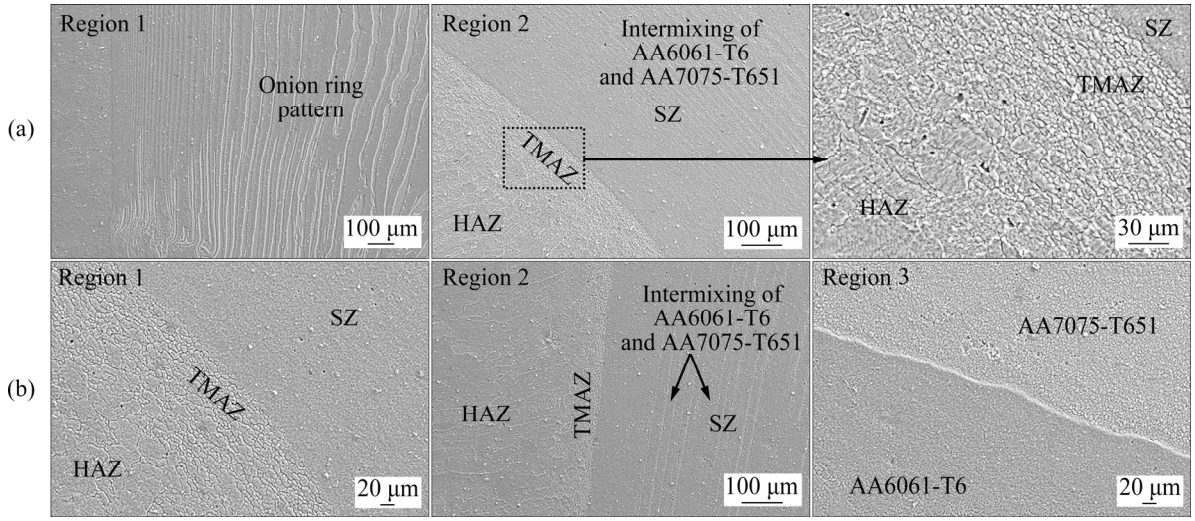

Fig. 4 FE-SEM images of different regions on cross-section of AA6061−AA7075 FSW joint obtained using cylindrical tool pin with eccentricity of 0.5 mm: (a) Without preheating (referring to Fig. 2(b) for locations of Regions 1 and 2); (b) With preheating (referring to Fig. 2(b) for locations of Regions 1, 2 and 3)

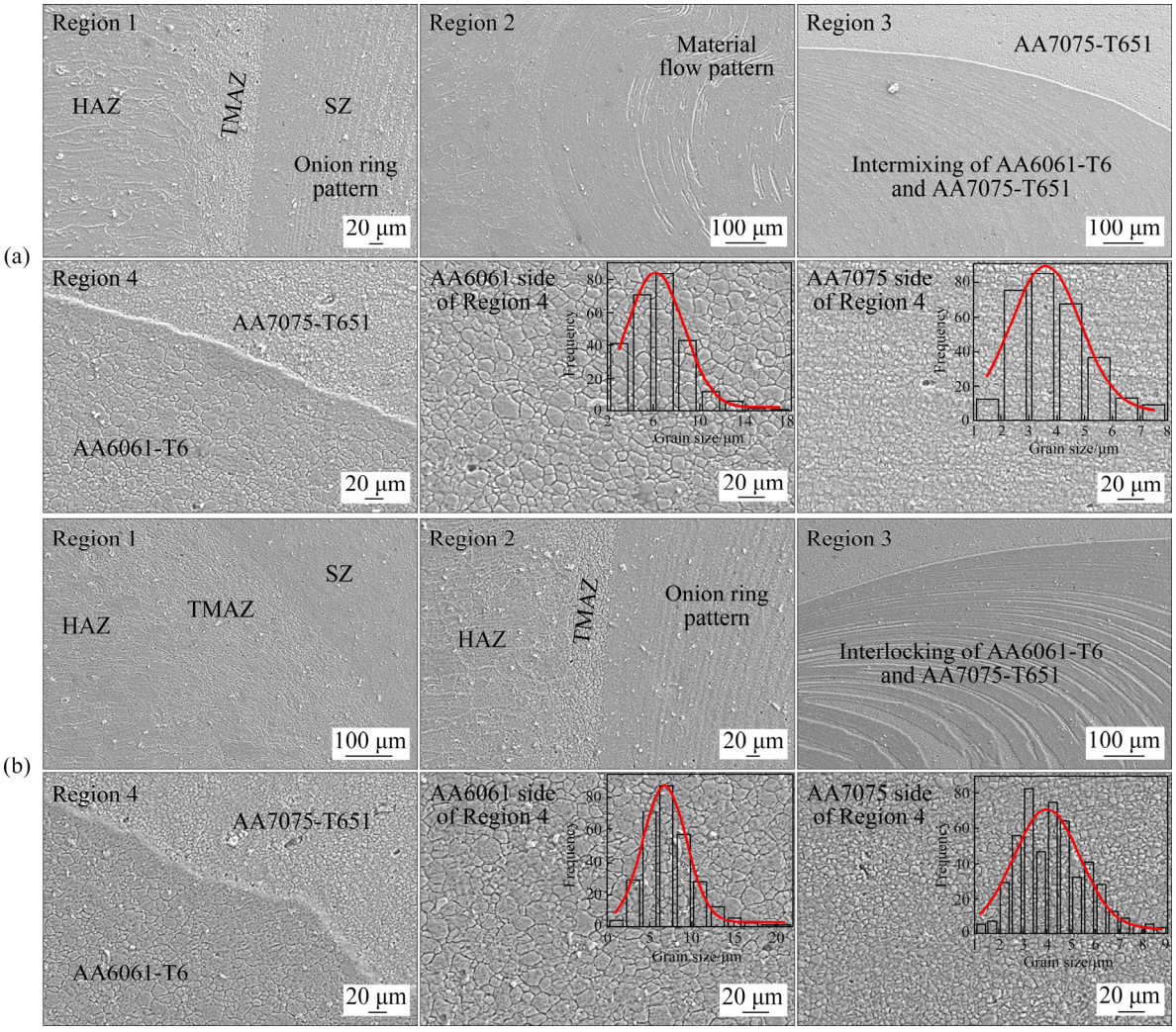

Fig. 5 FE-SEM images of different regions on cross-section of AA6061−AA7075 FSW joint obtained using cylindrical tool pin with eccentricity of 1 mm: (a) Without preheating (referring to Fig. 2(c) for locations of Regions 1, 2, 3 and 4); (b) With preheating (referring to Fig. 2(c) for locations of Regions 1, 2, 3 and 4)

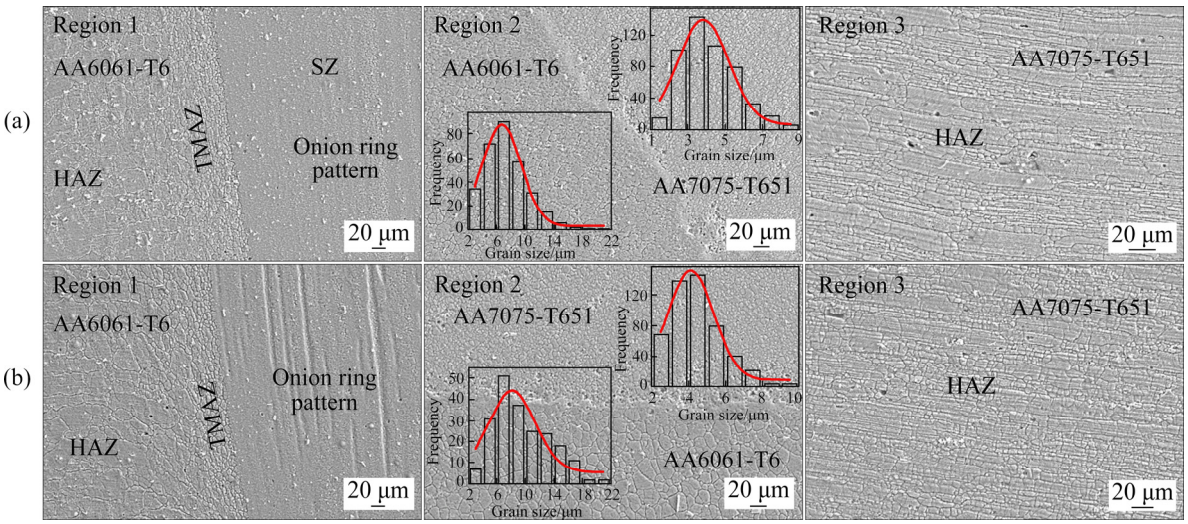

Fig. 6 FE-SEM images of different regions on cross-section of AA6061−AA7075 FSW joint obtained using square tool pin: (a) Without preheating (referring to Fig. 2(d) for locations of Regions 1, 2 and 3); (b) With preheating (referring to Fig. 2(d) for locations of Regions 1, 2 and 3)

respectively in AA6061 and AA7075 regions. Alike, for other tool pins in square tool pin, the grain size also slightly increases when preheating is employed during welding. The grain size in SZ of joint prepared with additional heating is measured to be 8.14 μm (in AA6061-T6) and 4.11 μm (in AA7075-T651) respectively.

Figure 7 shows the variation of the recorded vibro-

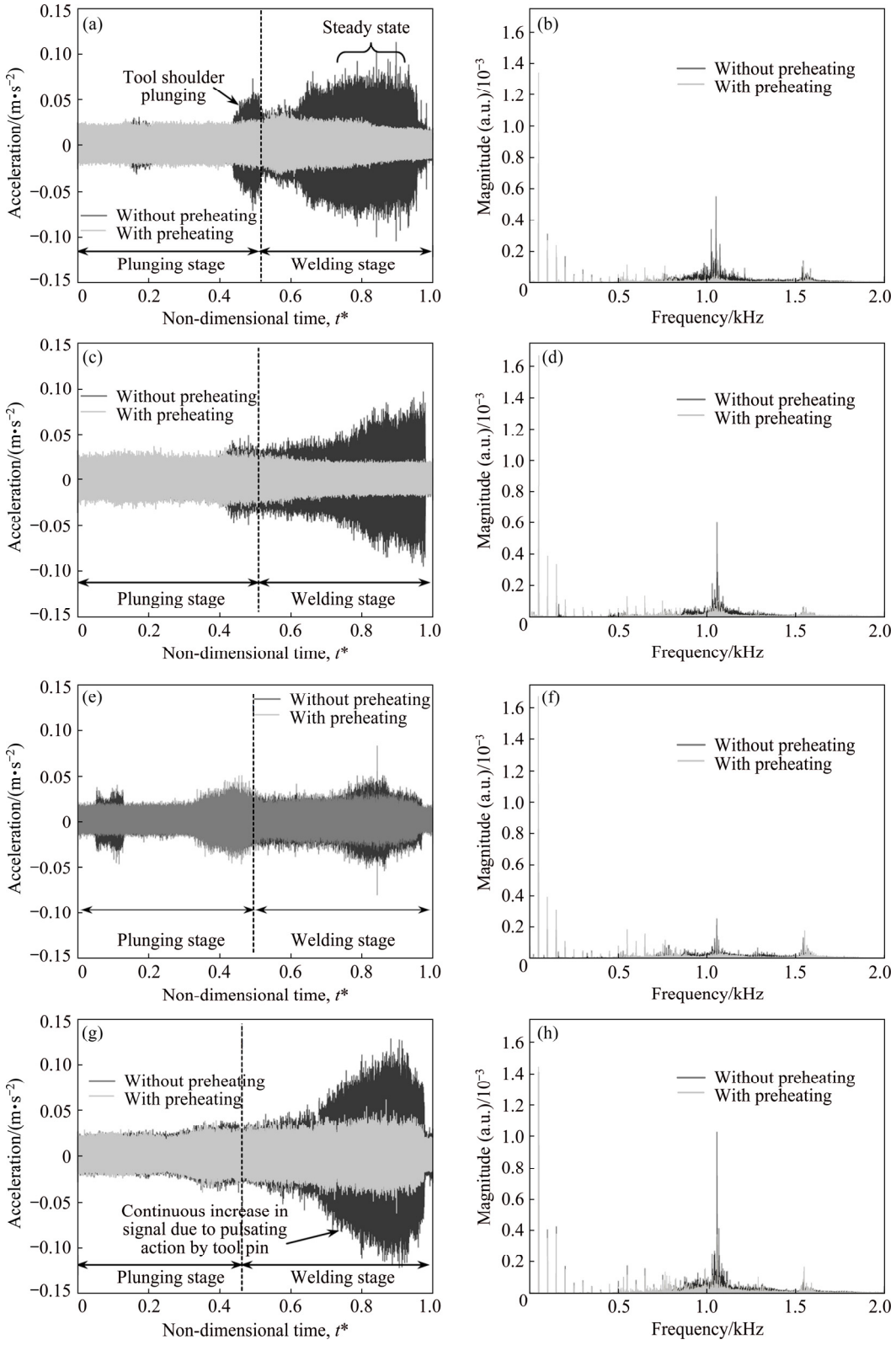

Fig. 7 Measured vibro-acoustic signal in time domain (a, c, e, g), and converted signal to frequency domain (b, d, f, h) during FSW of AA6061−AA7075 alloys with cylindrical tool pin (a, b), cylindrical tool pin with eccentricity of 0.5 mm (c, d), cylindrical tool pin with eccentricity of 1 mm (e, f) and square tool pin (g, h) without and with preheating

acoustic signal in Z direction versus non-dimensional time ($t_i^*=(t_i-t_{min})/(t_{max}-t_{min})$, where t_i is the instantaneous time; t_{min} is the minimum time and t_{max} is the maximum time for a particular welding) and the corresponding Fast Fourier Transform (FFT) in frequency domain for welded joints prepared with different tool pins and without as well as with preheating. Figure 7 shows that the magnitude of the vibro-acoustic signal remains almost uniform during plunging of the tool pin into the workpiece. However, a slight decrease in the magnitude of signal is also observed, which may be expected due to mild softening of workpiece material. A sudden increase in acoustic signal is observed when the tool shoulder touches the workpiece and additional region undergoes plastic deformation that also contributes to the increase in temperature due to the increase in frictional contact between the workpiece and tool surface. A mild drop in signal is noticed when the tool shoulder reaches the desired depth and tool plunging stops to initiate transverse in the forward direction (welding stage). Also with the start of tool movement in the welding direction the vibro-acoustic signal increases as tool experiences the frictional resistance while moving in welding direction. However, soon acoustic signal reaches almost steady state (Fig. 7(a)) due to steady heat generation and softening of material. From Fig. 7 it can also be seen that for eccentric tool pin less magnitude of signal is observed (minimum for 1 mm eccentric tool pin). As eccentric tool pin sweep plasticized material during each rotation that causes the temperature rise of the workpiece material due to severe plastic deformation as well as friction, with the increase in temperature and subsequent softening of base material the resistance to the tool by the workpiece decreases and possibly less extrusion force is required to move the low viscosity plasticized material.

It may also be noted from Fig. 7(g) that for square tool pin, the magnitude of signal is comparatively higher than cylindrical tool pins. This increase in signal could be due to frictional contact between tool and workpiece surface and moreover, the square tool pin sweeps high viscosity material under pulsating/extrusion action of tool rotation. Therefore, square tool pin experiences frictional resistance while moving forward through undeformed material. Figure 7 also shows that with additional heating the magnitude of vibro-acoustic signal significantly drops for different tool pins. This drop in vibro-acoustic signal with preheating can be associated with the high heat input which causes high degree of deformation and easy flow of plasticized material around the tool pin surface. Figure 7 also shows the vibro-acoustic signal converted into frequency domain using FFT, which indicates that the pattern of frequency bands with almost similar trend for different tool pins but of different magnitudes. This is mainly due to the variation in contact region between the tool and workpiece surfaces and stirring action by tool pins. It may also be noted from Fig. 7 that the magnitude of frequency bands drops after preheating, which is mainly associated with the drop in vibro-acoustic signal in time domain.

To evaluate the influence of pin profiles and pin eccentricity on the performance of joints, tensile strength and flexural load were measured for FSW joints and the variations are shown in Fig. 8. The tensile strength and flexural load of welded joints obtained with eccentric tool pins are observed to be higher (maximum for 1 mm eccentric pin) when compared to concentric tool pins. This may be due to the fact that the eccentric tool pin sweeps larger volume of plasticized material during rotation which forms a wider stir zone, enhances heat input, degree of deformation and flowability of plasticized material. For welded joints obtained with square tool pin, the tensile strength and flexural load are also observed to be higher than those obtained with concentric cylindrical tool pin. Figures 8(a) and (b) also show that the tensile strength and flexural load are

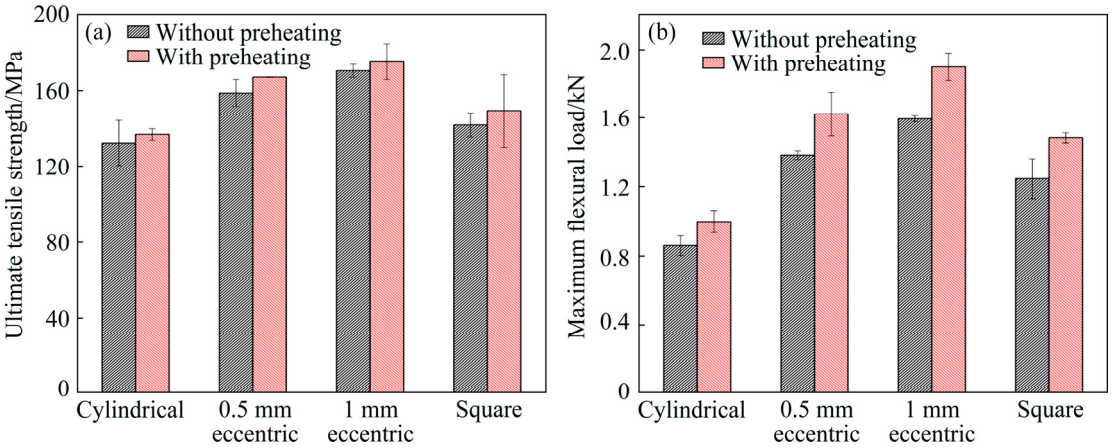

Fig. 8 Comparison of ultimate tensile strength (a) and maximum flexural load at failure (b) for AA6061−AA7075 FSW joints prepared with different tool pin profiles

significantly improved when the specimen is preheated with additional heating. Preheating provides the additional heat input which improves the material flow, deformation and bond strength between welded joints.

4 Conclusions

(1) The eccentric tool pins provided good flowability and intermixing between AA7075−AA6061 dissimilar alloys and a wider stir zone was formed. Grain size distributions in stir zone were also observed to be sufficiently finer with eccentric tool pin than that with concentric tool pin.

(2) The additional heating prior and during the welding stage provided better mixing and joining between dissimilar alloys and also the grain size and size of stir zone were slightly coarsened.

(3) Different vibro-acoustic signal patterns were observed when different tool pin profiles were used and for all cases, the magnitude of the signal was higher during welding stage compared to the plunging stage. The signal was more steady and uniform for concentric cylindrical tool pin than that for square tool pin.

(4) Preheating significantly reduced the vibro-acoustic signal due to softening and easy flow of plasticized material around the tool surface.

(5) The maximum joint tensile and flexural strengths were observed for joints prepared with 1 mm eccentric cylindrical tool pin compared to other cases. For concentric tool pins, square tool pin provided higher joint strength than cylindrical pin. Tensile and flexural strengths of welded joints were slightly improved when specimen was preheated with additional heating.

Acknowledgement

Authors acknowledge the financial support received from Science and Engineering Research Board (SERB) of DST, New Delhi, India, for the present work (project number: YSS/2015/000085).

References

[1] ÇAM G, MISTIKOĞLU S. Recent developments in friction stir welding of Al-alloys [J]. Journal of Materials Engineering and Performance, 2014, 23: 1936−1953.

[2] ÇAM G, İPEKOĞLU G, KÜÇÜKÖMEROĞLU T, AKTARER S M. Applicability of friction stir welding to steels [J]. Journal of Achievements in Materials and Manufacturing Engineering, 2017, 80(2): 65−85.

[3] ÇAM G. Friction stir welded structural materials: Beyond Al-alloys [J]. International Materials Reviews, 2011, 56(1): 1−48.

[4] KASHAEV N, VENTZKE V, ÇAM G. Prospects of laser beam welding and friction stir welding processes for aluminum airframe structural applications [J]. Journal of Manufacturing Processes, 2018, 36: 571−600.

[5] RATURI M, GARG A, BHATTACHARYA A. Joint strength and failure studies of dissimilar AA6061−AA7075 friction stir welds: Effects of tool pin, process parameters and preheating [J]. Engineering Failure Analysis, 2019, 96: 570−588.

[6] VERMA J, TAIWADE R V, REDDY C, KHATIRKAR R K. Effect of friction stir welding process parameters on Mg−AZ31B/Al−AA6061 joints [J]. Materials and Manufacturing Processes, 2018, 33(3): 308−314.

[7] SHANAVAS S, EDWIN RAJA DHAS J. Parametric optimization of friction stir welding parameters of marine grade aluminium alloy using response surface methodology [J]. Transactions of Nonferrous Metals Society of China, 2017, 27: 2334−2344.

[8] SHARMA C, UPADHYAY V, DWIVEDI D K, KUMAR P. Mechanical properties of friction stir welded armor grade Al−Zn−Mg alloy joints [J]. Transactions of Nonferrous Metals Society of China, 2017, 27: 493−506.

[9] DAWOOD H I, MOHAMMED K S, RAHMAT A, UDAY M B. Effect of small tool pin profiles on microstructures and mechanical properties of 6061 aluminum alloy by friction stir welding [J]. Transactions of Nonferrous Metals Society of China, 2015, 25: 2856−2865.

[10] YANG Min, BAO Rui-jun, LIU Xiu-zhong, SONG Chao-qun. Thermo-mechanical interaction between aluminum alloy and tools with different profiles during friction stir welding [J]. Transactions of Nonferrous Metals Society of China, 2019, 29: 495−506.

[11] YADUWANSHI D K, BAG S, PAL S. On the effect of tool offset in hybrid-FSW of copper−aluminium alloy [J]. Materials and Manufacturing Processes, 2018, 33(3): 277−287.

[12] JAYABALAKRISHNAN D, BALASUBRAMANIAN M. Eccentric-weave FSW between Cu and AA6061-T6 with reinforced graphene nanoparticles [J]. Materials and Manufacturing Processes, 2018, 33(3): 333−342.

[13] AMINI S, AMIRI M R. Pin axis effects on forces in friction stir welding process [J]. The International Journal of Advanced Manufacturing Technology, 2015, 78: 1795−1801.

[14] MAO Y Q, KE L M, LIU F C, LIU Q, HUANG C P, LI X. Effect of tool pin eccentricity on microstructure and mechanical properties in friction stir welded 7075 aluminum alloy thick plate [J]. Materials and Design, 2014, 62: 334−343.

[15] SHAH L H, GUO S, WALBRIDGE S, GERLICH A. Effect of tool eccentricity on the properties of friction stir welded AA6061 aluminum alloys [J]. Manufacturing Letters, 2018, 15: 14−17.

[16] CHEN Y, WANG H, WANG X, DING H, ZHAO J, ZHANG F, REN Z. Influence of tool pin eccentricity on microstructural evolution and mechanical properties of friction stir processed Al-5052 alloy [J]. Materials Science and Engineering A, 2019, 739: 272−276.

[17] BANG H S, BANG H S, JEON G H, OH I H, RO C S. Gas tungsten arc welding assisted hybrid friction stir welding of dissimilar materials Al6061-T6 aluminum alloy and STS304 stainless steel [J]. Materials and Design, 2012, 37: 48−55.

[18] YADUWANSHI D K, BAG S, PAL S. Effect of preheating in hybrid friction stir welding of aluminum alloy [J]. Journal of Materials Engineering and Performance, 2014, 23: 3794−3803.

[19] SINCLAIR P C, LONGHURST W R, COX C D, LAMMLEIN D H, STRAUSS A M, COOK G E. Heated friction stir welding: An experimental and theoretical investigation into how preheating influences process forces [J]. Materials and Manufacturing Processes, 2010, 25: 1283−1291.

[20] İPEKOĞLU G, ERİM S, ÇAM G. Investigation into the influence of post-weld heat treatment on the friction stir welded AA6061 Al-alloy plates with different temper conditions [J]. Metallurgical and Materials Transaction A, 2014, 45: 864−877.

[21] İPEKOĞLU G, ERİM S, ÇAM G. Effects of temper condition and post weld heat treatment on the microstructure and mechanical properties of friction stir butt-welded AA7075 Al alloy plates [J]. The

International Journal of Advanced Manufacturing Technology, 2014, 70: 201−213.

[22] İPEKOĞLU G, ÇAM G. Effects of initial temper condition and postweld heat treatment on the properties of dissimilar friction-stir-welded joints between AA7075 and AA6061 aluminum alloys [J]. Metallurgical and Materials Transaction A, 2014, 45: 3074−3087.

[23] SAFARBALI B, SHAMANIAN M, ESLAMI A. Effect of post-weld heat treatment on joint properties of dissimilar friction stir welded 2024-T4 and 7075-T6 aluminum alloys [J]. Transactions of Nonferrous Metals Society of China, 2018, 28: 1287−1297.

[24] ÇAM G, İPEKOĞLU G, SERINDAĞ H T. Effects of use of higher strength interlayer and external cooling on properties of friction stir welded AA6061-T6 joints [J]. Science and Technology of Welding and Joining, 2014, 19(8): 715−720.

[25] DONATUS U, THOMPSON G E, MOMOH M I, MALEDI N B, TSAI I L, OLIVEIRA FERREIRA R, LIU Z. Variations in stir zone and thermomechanically affected zone of dissimilar friction stir weld of AA5083 and AA6082 alloys [J]. Transactions of Nonferrous Metals Society of China, 2018, 28: 2410−2418.

[26] CHEN C, KOVACEVIC R, JANDGRIC D. Wavelet transform analysis of acoustic emission in monitoring friction stir welding of 6061 aluminum [J]. International Journal of Machine Tools and Manufacture, 2003, 43: 1383−1390.

[27] SENTHILKUMAR S, NARAYANAN S, DENIS A S. Acoustic emission-based monitoring approach for friction stir welding of aluminum alloy AA6063-T6 with different tool pin profiles [J]. Proceedings of the Institution of Mechanical Engineers, Part B: Journal of Engineering Manufacture, 2013, 227: 407−416.

[28] FERNÁNDEZ J B, ROCA A S, FALS H C, MACÍAS E J, de LA PARTE M P. Application of vibroacoustic signals to evaluate tools profile changes in friction stir welding on AA 1050 H24 alloy [J]. Science and Technology of Welding and Joining, 2012, 17(6): 501−510.

[29] MACÍAS E J, ROCA A S, FALS H C, MURO J C S, FERNÁNDEZ J B. Characterisation of friction stir spot welding process based on envelope analysis of vibro-acoustical signals [J]. Science and Technology of Welding and Joining, 2015, 20(2): 172−180.

[30] SOUNDARARAJAN V, ATHARIFAR H, KOVACEVIC R. Monitoring and processing the acoustic emission signals from the friction-stir-welding process [J]. Proceedings of the Institution of Mechanical Engineers, Part B: Journal of Engineering Manufacture, 2006, 220: 1673−1685.

[31] OROZCO M S, MACÍAS E J, ROCA A S, FALS H C, FERNÁNDEZ J B. Optimisation of friction-stir welding process using vibro-acoustic signal analysis [J]. Science and Technology of Welding and Joining, 2013, 18(6): 532−540.

[32] RAJAPRAKASH B M, SURESHA C N, RACHAPPA, UPADHYA S. Application of acoustic emission technique for online monitoring of friction stir welding process during welding of AA6061-T6 aluminum alloy [C]//Supplemental Proceedings 2014. Pittsburgh, PA: TMS, 2014: 731−740.

[33] MURTHY V, ULLEGADDI K, MAHESH B, RAJAPRAKASH B M. Application of image processing and acoustic emission technique in monitoring of friction stir welding process [J]. Materials Today: Proceedings, 2017, 4: 9186−9195.

预热辅助搅拌摩擦焊 AA6061-T6 和 AA7075-T651 合金的冶金性能和振声信号变化

Ashu GARG, Madhav RATURI, Anirban BHATTACHARYA

Department of Mechanical Engineering, Indian Institute of Technology Patna, Bihar, India

摘　要：研究 AA6061-T6 和 AA7075-T651 合金在搅拌摩擦焊接(FSW)过程中搅拌头形状(圆柱形和方形)、圆柱形搅拌头偏心距(0.5 mm 和 1mm)和预热(二次加热)对合金冶金性能、振声信号波形变化和接头强度的影响。观察到偏心针能提供良好的流动性和异种金属间的混合，增大搅拌区尺寸，细化搅拌区晶粒尺寸。当轴肩突然插入时，振声信号强度增加；当轴肩到达所需深度时，信号强度减小。与搅拌头插入过程相比，在焊接过程中产生的信号强度更高，这是由于搅拌头在沿焊接轨道运动过程中会不断吸收新的材料。在搅拌针插入前和焊接过程中对工件进行预热可显著影响焊料流动行为和混合形式。与未预热的样品相比，预热后样品中搅拌区的晶粒更粗大，且预热后信号强度明显下降。采用额外加热后，焊接接头的拉伸强度和抗弯强度略有提高。

关键词：搅拌摩擦焊；搅拌头形状；偏心盘；预热；振声信号；显微组织；强度

(Edited by Wei-ping CHEN)